AIMS Mathematics, 11(4): 12064–12093.
DOI: 10.3934/math.2026495
Received: 05 March 2026
Revised: 07 April 2026
Accepted: 10 April 2026
Published: 29 April 2026

https://www.aimspress.com/journal/Math

Research article

Classical and Bayesian inference for progressively censored competing risks data under the Gompertz-Lindley model

Mahmoud H. Abu-Moussa[1,2], Ehab M. Almetwally[3,*] and Abd El-Raheem M. Abd El-Raheem[4]

[1] Department of Mathematics, Faculty of Science, Cairo University, Giza, Egypt
[2] Faculty of Education and Arts, Sohar University, Sohar, Oman
[3] Department of Mathematics and Statistics, College of Science, Imam Mohammad Ibn Saud Islamic University (IMSIU), Riyadh 11432, Saudi Arabia
[4] Department of Mathematics, Faculty of Education, Ain Shams University, Cairo, Egypt

* **Correspondence:** Email: emalmetwally@imamu.edu.sa.

Abstract: This paper develops classical and Bayesian inferential procedures for progressively Type-II censored competing-risks data when the latent failure times follow the Gompertz-Lindley distribution. Maximum likelihood estimators are derived for the model parameters, and asymptotic confidence intervals are constructed using the observed information matrix. Bayesian estimation is carried out under squared error, LINEX, and generalized entropy loss functions using both the Tierney–Kadane approximation and Markov chain Monte Carlo methods. An extensive Monte Carlo simulation study is conducted to assess the finite-sample behavior of the proposed estimators under different sample sizes and progressive censoring schemes. The numerical results show that Bayesian procedures generally outperform the corresponding maximum likelihood estimators, particularly in small and moderately censored samples. A real-data application involving heart-disease patients demonstrates that the Gompertz-Lindley model provides a satisfactory fit and serves as a flexible alternative for competing-risks lifetime data.

Keywords: progressive Type-II censoring; competing risks modeling; Gompertz-Lindley lifetime model; Bayesian estimation techniques; statistical survival analysis
Mathematics Subject Classification: 62F15, 62N05

1. Introduction

In time-to-event analysis, competing risks occur when an individual or unit is subject to multiple, mutually exclusive failure types, such that the occurrence of one event prevents the observation of the remaining events. This situation is frequently encountered in many applied fields. For example, in

cancer survival studies, cancer death may be the event of interest, whereas non-cancer death is a competing risk because it prevents cancer death from occurring later. Treating non-cancer death as ordinary censoring overestimates cancer-specific mortality. In engineering, a component may fail by corrosion, thermal fatigue, or another mechanism; the first one to occur determines failure, see for example [28–30].Ignoring competing mechanisms can potentially bias the estimation of the target failure mode and affect the assessment of overall reliability. Similarly, in actuarial science, insurance claims may arise from different underlying causes. Ignoring the presence of competing risks and applying standard survival analysis techniques can result in biased and potentially misleading conclusions, as traditional methods typically rely on the assumption of noninformative censoring. In contrast, competing risks settings require specialized inferential frameworks that appropriately account for the dependence between event types and enable the accurate estimation of fundamental quantities, such as the cumulative incidence function, which represents the probability of failure from a specific cause over time. Parametric competing risks models commonly assume that the latent failure times associated with each cause follow specified probability distributions, including the Weibull, exponential, log-normal, or generalized gamma distributions. Because only the earliest failure time is observed, the joint modeling of cause-specific failure times must properly accommodate informative censoring. A classical approach involves specifying parametric models for the cause-specific hazard functions and constructing the likelihood accordingly. Alternatively, one may model the observed failure time as the minimum of latent event times with known distributions, often assuming independence among causes or introducing copula-based structures to capture potential dependence see (Crowder [11] and Geskus [13]).

Research on competing risks within survival analysis has developed substantially over time, originating from the seminal work of Cox [10], who investigated exponentially distributed lifetimes in the presence of multiple failure causes and laid the methodological foundations for competing risks modeling. Subsequently, Crowder [11] provided a rigorous classical treatment, with particular emphasis on likelihood-based inference and parametric model construction. Kalbfleisch and Prentice [19] later presented a comprehensive statistical framework for failure time analysis, encompassing both nonparametric and parametric methodologies for competing risks data. An important advancement in parametric inference was introduced by Kundu et al. [22], who explored competing risks models under progressive censoring, demonstrating enhanced flexibility in accommodating complex censoring schemes. Almetwally et al. [7] discussed the regression competing risks model with an application to HIV and AIDS infection. Koley and Kundu [20] developed inferential procedures for generalized progressive hybrid censoring, enabling more robust analysis under intricate censoring structures and multiple risk settings. Extending this line of research, Ramadan et al. [26] proposed inferential methods for the parameters of the Akshaya distribution under competing-risks data and illustrated their approach with an application to HIV-AIDS patient data. Aboul-Fotouh et al. [2] developed inferential procedures for generalized progressive hybrid Type-II censored Weibull lifetimes under competing-risks data, proposing estimation and hypothesis-testing methods tailored to the complex censoring and multiple-cause framework. Haj Ahmad et al. [15] investigated competing risks within accelerated life-testing, developing step-stress models that incorporate tampered random variables to better capture stress-dependent failure behavior. More contributions to the competing risks literature include the works of Koley and Kundu [21], Abd El-Raheem et al. [1], Mahto [23], Nassr et al. [24], and Hassan et al. [16–18], which

further advanced methodological developments and applications in competing risks. El-Azeem et al. [12] discussed the competing risks model under the step-strength accelerated life testing.

Progressive Type-II censoring represents a flexible and efficient censoring mechanism that has been widely adopted in life-testing and reliability studies, particularly in situations where experimental units are intentionally removed during the test to reduce cost, time, or operational constraints. Under this scheme, a fixed number of failures is observed, and at each observed failure time, a prespecified number of surviving units is randomly withdrawn from the experiment. This design enables investigators to balance the acquisition of informative failure data with practical resource limitations. The progressive Type-II censoring model was formally introduced by Balakrishnan and Aggarwala [8] and has since become a fundamental tool in statistical inference for reliability and survival analysis. Owing to its inherent flexibility and efficiency, the scheme has gained increasing prominence in parametric inference, model discrimination, and Bayesian analysis, particularly within contemporary industrial and biomedical applications (see Balakrishnan and Cramer [9]). Moreover, progressive Type-II censoring has proven especially effective in addressing more complex inferential settings, including competing risks and hybrid censoring frameworks.

Mathematically, the progressive Type-II censoring scheme is described as follows. Suppose that n identical units are placed on a life test, with the objective of observing exactly m failures, where $m < n$. The censoring is implemented sequentially: immediately after the occurrence of the first failure, R_1 of the remaining units are randomly removed from the experiment; following the second failure, an additional R_2 units are withdrawn, and this procedure continues in a similar manner. At the time of the mth failure, the remaining R_m units are censored. The censoring scheme is constrained by the condition $R_1 + R_2 + \cdots + R_m = n - m$.

This study focuses on the problem of statistical inference (SI) for a competing-risks framework in which the latent failure times are assumed to follow the Gompertz-Lindley distribution (GLD). The GLD, parameterized by α and β, was originally introduced by Ghitany et al. [14]. The corresponding probability density function (PDF), survival function (SF), and hazard rate function (HRF) are respectively expressed as follows:

$$f(t) = \frac{\alpha^2\beta e^{\beta t}[e^{\beta t} + \alpha + 1]}{(\alpha + 1)[e^{\beta t} + \alpha - 1]^3}, \quad t > 0, \ \alpha, \beta > 0, \tag{1.1}$$

$$\overline{F}(t) = \frac{\alpha^2[e^{\beta t} + \alpha]}{(\alpha + 1)[e^{\beta t} + \alpha - 1]^2}, \quad t > 0, \tag{1.2}$$

and

$$H(t) = \frac{\beta e^{\beta t}[e^{\beta t} + \alpha + 1]}{(e^{\beta t} + \alpha)[e^{\beta t} + \alpha - 1]}, \quad t > 0. \tag{1.3}$$

The GLD was proposed as a flexible lifetime model that integrates key characteristics of the Gompertz and Lindley distributions. This composite structure enhances its ability to model positively skewed lifetime data and has been shown to yield superior goodness-of-fit performance in a variety of survival and reliability applications. A notable feature of the GLD is its capacity to accommodate diverse hazard rate shapes, including increasing, decreasing, and unimodal forms; see Figure 1, which makes it particularly well-suited for engineering and biomedical studies involving complex and heterogeneous failure mechanisms. In addition, the GLD model admits analytically tractable inferential procedures, thereby facilitating both classical and Bayesian analyses. Owing to these

advantageous properties, the GLD has attracted growing attention in the recent literature and has emerged as a competitive alternative to traditional lifetime models [14]. Recent methodological and applied developments involving the GLD can be found in [3, 4].

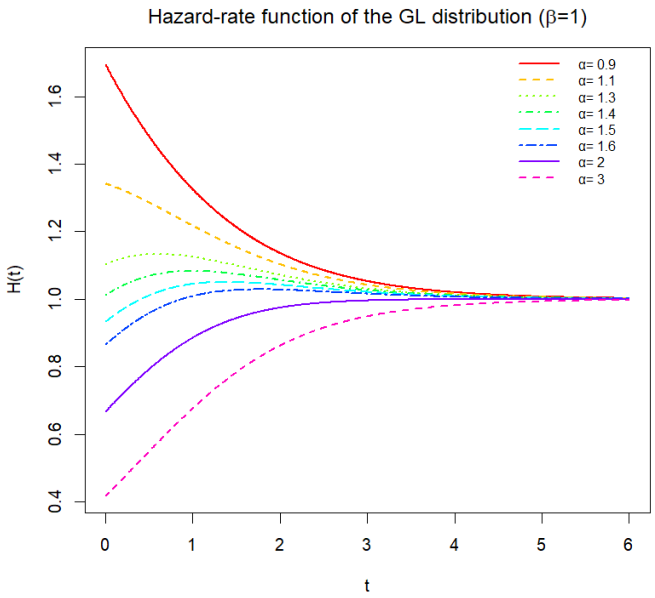

Figure 1. Hazard-rate function of the GLD for selected values of α and $\beta = 1$.

The principal aim of this study is to develop a comprehensive statistical inference framework for the GLD under progressive Type-II censoring in the presence of competing risks. In particular, the study seeks to construct and examine estimation procedures that enable reliable inference on the underlying distributional parameters when multiple, mutually exclusive failure causes are present and lifetime observations are only partially available due to censoring. To this end, several point estimation methodologies are developed and evaluated, including maximum likelihood estimation and alternative estimation approaches suited to progressively censored competing risks (PC-CR) data. A further objective is to assess the empirical performance of these inferential procedures through simulation and real-data applications, thereby determining the suitability and robustness of the GLD relative to established lifetime models. Collectively, the study seeks to expand the methodological tools available for analyzing complex survival data and to support the GLD as a viable model in reliability, biostatistics, and related disciplines.

The article presents and precisely develops inferential procedures for the GLD within the framework of progressive type-II censoring when multiple competing causes of failure are present. To the best of our knowledge, no prior work has addressed the GLD model under progressively censored competing risks schemes, thereby expanding the applicability of the distribution to a new class of survival investigations. The remainder of this article is structured as follows. Section 2 outlines the progressive Type-II censoring scheme in the presence of competing risks and presents the associated notation. Section 3 derives the maximum likelihood estimators for the model parameters and provides asymptotic confidence intervals for the parameters of the GLD under PC-CR data. Section 4 develops the Bayesian estimators and their Markov chain Monte Carlo (MCMC) approximations, along with credible intervals constructed under various loss functions, including squared error, LINEX, and

generalized entropy losses. Furthermore, Bayesian point estimation is carried out using the Tierney-Kadane approximation, which provides a highly accurate second-order Laplace approximation to posterior moments without the computational burden of simulation-based methods. Section 5 reports the results of an extensive simulation study conducted to evaluate the finite-sample performance of the estimators. Section 6 suggests a numerical analysis based on a real data set to illustrate the applicability of the presented methodology. Finally, Section 7 offers concluding remarks and possible recommendations for future research.

2. Model and notations

This section presents the competing risks framework together with the associated notation. Consider an experiment involving n units that may fail due to two known causes of failure. For each unit $i = 1, 2, \ldots, n$, define

$T_i = \min\{T_{i1}, T_{i2}\}$, where T_{ij} denotes the latent failure time of the ith unit attributable to the jth cause, $j = 1, 2$. The latent failure times T_{i1} and T_{i2} are independent and follow GLD(α, β_1) and GLD(α, β_2) distributions, respectively. Furthermore, the pairs (T_{i1}, T_{i2}), $i = 1, 2, \ldots, n$, are assumed to constitute an independent and identically distributed collection of random variables.

Let $X_1 \sim$ GLD(α, β_1) and $X_2 \sim$ GLD(α, β_2) be independent. Then, the SF of the random variable, $X = \min\{X_1, X_2\}$, is given by

$$\overline{G}(x; \alpha, \beta_1, \beta_2) = \frac{\alpha^4 (e^{\beta_1 x} + \alpha)(e^{\beta_2 x} + \alpha)}{(\alpha + 1)^2 (e^{\beta_1 x} + \alpha - 1)^2 (e^{\beta_2 x} + \alpha - 1)^2}. \tag{2.1}$$

Consequently, the cumulative distribution function and PDF of X are given respectively by

$$G(x; \alpha, \beta_1, \beta_2) = 1 - \frac{\alpha^4 (e^{\beta_1 x} + \alpha)(e^{\beta_2 x} + \alpha)}{(\alpha + 1)^2 (e^{\beta_1 x} + \alpha - 1)^2 (e^{\beta_2 x} + \alpha - 1)^2}, \tag{2.2}$$

and

$$\begin{aligned} g(x; \alpha, \beta_1, \beta_2) = & \frac{\alpha^4}{(\alpha + 1)^2 \left(\alpha + e^{\beta_1 x} - 1\right)^3 \left(\alpha + e^{\beta_2 x} - 1\right)^3} \left(\left(2\alpha^2 + \alpha - 1\right)(\beta_1 + \beta_2) e^{(\beta_1 + \beta_2)x} \right. \\ & + \alpha \left(\alpha^2 - 1\right) \beta_1 e^{\beta_1 x} + \alpha \left(\alpha^2 - 1\right) \beta_2 e^{\beta_2 x} + (2\alpha\beta_1 + \alpha\beta_2 - \beta_1 + \beta_2) e^{(2\beta_1 + \beta_2)x} \\ & + (\alpha\beta_1 + 2\alpha\beta_2 + \beta_1 - \beta_2) e^{(\beta_1 + 2\beta_2)x} + (\alpha - 1)\alpha\beta_1 e^{2\beta_1 x} + (\alpha - 1)\alpha\beta_2 e^{2\beta_2 x} + (\beta_1 \\ & \left. + \beta_2) e^{2(\beta_1 + \beta_2)x} \right). \end{aligned} \tag{2.3}$$

To describe the progressively Type-II censored competing risks data, assume that n identical units are placed on test according to a predetermined censoring scheme $\mathcal{R} = (R_1, R_2, \ldots, R_m)$. In this setup, m denotes the total number of observed failures, and $n - m$ units are censored. At the time of the ith failure, R_i surviving units are randomly withdrawn from the experiment. For each observed failure, the cause is recorded; if the ith failure is attributed to the jth risk, we set $\delta_i = j$. Thus, $m_j = \sum_{i=1}^{m} I(\delta_i = j)$, represents the number of failures attributable to cause j, so that $m = m_1 + m_2$, where

$$I(\delta_i = j) = \begin{cases} 1, & \delta_i = j, \\ 0, & \text{otherwise.} \end{cases}$$

Based on the preceding specification, the joint PDF of the observed data $\mathbf{T} = (T_1, T_2, \ldots, T_m)$ is given by [22]:

$$L(\mathbf{T}) = n \prod_{i=1}^{m-1} \left(n - \sum_{k=1}^{i} (R_k + 1) \right) \prod_{i=1}^{m} \prod_{j=1}^{2} \left(f_j(t_i) \overline{F}_{3-j}(t_i) \right)^{I(\delta_i = j)} \left(\overline{F}_1(t_i) \overline{F}_2(t_i) \right)^{R_i}, \tag{2.4}$$

where $\overline{F}_j(t_i)$ and $f_j(t_i)$ denote the SF and PDF associated with cause j at time t_i, for $i = 1, 2, \ldots, m$ and $j = 1, 2$.

3. Maximum likelihood estimation

The aim of this section is to obtain the maximum likelihood estimators (MLEs) for the unknown parameters of the GLD under PC-CR data. Using the notation introduced previously, the likelihood function for the parameters α, β_1, and β_2, denoted by $L(\alpha, \beta_1, \beta_2; t)$, takes the following form.

$$\begin{aligned} L(\alpha, \beta_1, \beta_2; t) = \frac{\alpha^{4m} \beta_1^{m_1} \beta_2^{m_2}}{(1+\alpha)^{2m}} \prod_{i=1}^{m} & \left(\frac{e^{\beta_1 t_i} \left(\alpha + e^{\beta_1 t_i} + 1 \right) \left(\alpha + e^{\beta_2 t_i} \right)}{(\alpha+1)^2 \left(\alpha + e^{\beta_1 t_i} - 1 \right)^3 \left(\alpha + e^{\beta_2 t_i} - 1 \right)^2} \right)^{I(\delta_i = 1)} \\ & \left(\frac{e^{\beta_2 t_i} \left(\alpha + e^{\beta_1 t_i} \right) \left(\alpha + e^{\beta_2 t_i} + 1 \right)}{(\alpha+1)^2 \left(\alpha + e^{\beta_1 t_i} - 1 \right)^2 \left(\alpha + e^{\beta_2 t_i} - 1 \right)^3} \right)^{I(\delta_i = 2)} \\ & \left(\frac{\left(\alpha + e^{\beta_1 t_i} \right) \left(\alpha + e^{\beta_2 t_i} \right)}{(\alpha+1)^2 \left(\alpha + e^{\beta_1 t_i} - 1 \right)^2 \left(\alpha + e^{\beta_2 t_i} - 1 \right)^2} \right)^{R_i}. \end{aligned} \tag{3.1}$$

Disregarding constant terms in Eq (3.1), the corresponding log-likelihood function (LLF) becomes

$$\begin{aligned} l \propto & \sum_{i=1}^{m} R_i \left(\log \left(\frac{\alpha^2 \left(\alpha + e^{\beta_1 t_i} \right)}{(\alpha+1) \left(\alpha + e^{\beta_1 t_i} - 1 \right)^2} \right) + \log \left(\frac{\alpha^2 \left(\alpha + e^{\beta_2 t_i} \right)}{(\alpha+1) \left(\alpha + e^{\beta_2 t_i} - 1 \right)^2} \right) \right) + \\ & \sum_{i=1}^{m} I(\delta_i = 1) \log \left(\frac{\alpha^4 \beta_1 e^{\beta_1 t_i} \left(\alpha + e^{\beta_1 t_i} + 1 \right) \left(\alpha + e^{\beta_2 t_i} \right)}{(\alpha+1)^2 \left(\alpha + e^{\beta_1 t_i} - 1 \right)^3 \left(\alpha + e^{\beta_2 t_i} - 1 \right)^2} \right) + \\ & \sum_{i=1}^{m} I(\delta_i = 2) \log \left(\frac{\alpha^4 \beta_2 e^{\beta_2 t_i} \left(\alpha + e^{\beta_1 t_i} \right) \left(\alpha + e^{\beta_2 t_i} + 1 \right)}{(\alpha+1)^2 \left(\alpha + e^{\beta_1 t_i} - 1 \right)^2 \left(\alpha + e^{\beta_2 t_i} - 1 \right)^3} \right). \end{aligned} \tag{3.2}$$

Differentiating the LLF with respect to α, β_1, and β_2 and equating the results to zero produces the following likelihood equations:

$$\begin{aligned} & \sum_{i=1}^{m} R_i \left(-\frac{2}{\alpha+1} + \frac{4}{\alpha} - \frac{2}{\alpha + e^{\beta_1 t_i} - 1} + \frac{1}{\alpha + e^{\beta_1 t_i}} - \frac{2}{\alpha + e^{\beta_2 t_i} - 1} + \frac{1}{\alpha + e^{\beta_2 t_i}} \right) \\ + & \sum_{i=1}^{m} I(\delta_i = 1) \left(-\frac{2}{\alpha+1} + \frac{4}{\alpha} - \frac{3}{\alpha + e^{\beta_1 t_i} - 1} + \frac{1}{\alpha + e^{\beta_1 t_i} + 1} - \frac{2}{\alpha + e^{\beta_2 t_i} - 1} + \frac{1}{\alpha + e^{\beta_2 t_i}} \right) \end{aligned}$$

$$+ \quad \sum_{i=1}^{m} I(\delta_i = 2)\left(-\frac{2}{\alpha+1} + \frac{4}{\alpha} - \frac{2}{\alpha+e^{\beta_1 t_i}-1} + \frac{1}{\alpha+e^{\beta_1 t_i}} - \frac{3}{\alpha+e^{\beta_2 t_i}-1} + \frac{1}{\alpha+e^{\beta_2 t_i}+1}\right) = 0, \tag{3.3}$$

$$\sum_{i=1}^{m} R_i\left(\frac{t_i e^{\beta_1 t_i}}{\alpha+e^{\beta_1 t_i}} - \frac{2t_i e^{\beta_1 t_i}}{\alpha+e^{\beta_1 t_i}-1}\right) + \sum_{i=1}^{m} I(\delta_i = 1)\left(\frac{1}{\beta_1} - \frac{3t_i e^{\beta_1 t_i}}{\alpha+e^{\beta_1 t_i}-1} + \frac{t_i e^{\beta_1 t_i}}{\alpha+e^{\beta_1 t_i}+1}\right)$$
$$+ \quad \sum_{i=1}^{m} I(\delta_i = 2)\left(\frac{t_i e^{\beta_1 t_i}}{\alpha+e^{\beta_1 t_i}} - \frac{2t_i e^{\beta_1 t_i}}{\alpha+e^{\beta_1 t_i}-1}\right) = 0, \tag{3.4}$$

and

$$\sum_{i=1}^{m} R_i\left(\frac{t_i e^{\beta_2 t_i}}{\alpha+e^{\beta_2 t_i}} - \frac{2t_i e^{\beta_2 t_i}}{\alpha+e^{\beta_2 t_i}-1}\right) + \sum_{i=1}^{m} I(\delta_i = 1)\left(\frac{1}{\beta_2} - \frac{3t_i e^{\beta_2 t_i}}{\alpha+e^{\beta_2 t_i}-1} + \frac{t_i e^{\beta_2 t_i}}{\alpha+e^{\beta_2 t_i}+1}\right)$$
$$+ \quad \sum_{i=1}^{m} I(\delta_i = 2)\left(\frac{t_i e^{\beta_2 t_i}}{\alpha+e^{\beta_2 t_i}} - \frac{2t_i e^{\beta_2 t_i}}{\alpha+e^{\beta_2 t_i}-1}\right) = 0. \tag{3.5}$$

Now, estimation is carried out by solving the likelihood Eqs (3.3)–(3.5) using the Newton-Raphson iterative procedure. Because the likelihood equations in (3.3)–(3.5) are nonlinear and do not realize closed-form solutions, the Newton-Raphson algorithm is implemented using data-driven initial values obtained from preliminary pilot estimates together with a coarse grid search over plausible positive parameter values. In all numerical investigations considered in this study, the iterative scheme converged to the same solution from a range of allowable starting points, indicating adequate numerical stability and suggesting that the resulting maximum likelihood estimates are not too sensitive to the initial values.

3.1. Asymptotic confidence intervals for the parameters

In this subsection, we construct asymptotic confidence intervals for the unknown parameter vector $\boldsymbol{\theta} = (\alpha, \beta_1, \beta_2)^\top$ of the GLD under PC-CR data. The proposed intervals are based on the large-sample properties of the MLEs. Under standard regularity conditions, the MLE $\widehat{\boldsymbol{\theta}}$ is asymptotically normally distributed as

$$\sqrt{m}\left(\widehat{\boldsymbol{\theta}} - \boldsymbol{\theta}\right) \xrightarrow{d} N_3\left(\mathbf{0}, \mathcal{I}^{-1}(\boldsymbol{\theta})\right), \tag{3.6}$$

where $\mathcal{I}(\boldsymbol{\theta})$ denotes the Fisher information matrix.

Because the analytical expressions of the second-order partial derivatives of the log-likelihood function $\ell(\boldsymbol{\theta})$ in Eq (3.2) are mathematically intractable, the Fisher information matrix is approximated using the observed information matrix, which is obtained from the Hessian matrix of $\ell(\boldsymbol{\theta})$ evaluated numerically at the MLE.

Specifically, the observed information matrix is given by

$$\mathcal{J}(\widehat{\boldsymbol{\theta}}) = -\left.\frac{\partial^2 \ell(\boldsymbol{\theta})}{\partial \boldsymbol{\theta}\, \partial \boldsymbol{\theta}^\top}\right|_{\boldsymbol{\theta}=\widehat{\boldsymbol{\theta}}}, \tag{3.7}$$

where the Hessian matrix is computed numerically.

The asymptotic variance–covariance matrix of $\widehat{\boldsymbol{\theta}}$ is then approximated by

$$\widehat{\Sigma} = \mathcal{J}^{-1}(\widehat{\boldsymbol{\theta}}). \tag{3.8}$$

Let $\widehat{\Sigma}_{jj}$ denote the jth diagonal element of $\widehat{\Sigma}$ corresponding to the parameter θ_j. Then, an asymptotic $(1-\gamma)\times 100\%$ confidence interval for θ_j is given by

$$\widehat{\theta}_j \ \pm \ z_{\gamma/2}\sqrt{\widehat{\Sigma}_{jj}}, \qquad j = 1, 2, 3, \tag{3.9}$$

where $z_{\gamma/2}$ is the upper $\gamma/2$ quantile of the standard normal distribution.

Accordingly, the asymptotic confidence intervals for the parameters α, β_1, and β_2 are obtained as

$$\widehat{\alpha} \ \pm \ z_{\gamma/2}\sqrt{\widehat{\mathrm{Var}}(\widehat{\alpha})}, \tag{3.10}$$

$$\widehat{\beta}_1 \ \pm \ z_{\gamma/2}\sqrt{\widehat{\mathrm{Var}}(\widehat{\beta}_1)}, \tag{3.11}$$

$$\widehat{\beta}_2 \ \pm \ z_{\gamma/2}\sqrt{\widehat{\mathrm{Var}}(\widehat{\beta}_2)}. \tag{3.12}$$

These confidence intervals are of the Wald type and rely on the asymptotic normality of MLEs. Their accuracy improves as the sample size increases, and their finite-sample performance is further evaluated through simulation studies in the subsequent section.

4. Bayesian estimation

In this section, Bayesian estimators (BEs) of the unknown parameters α, β_1, and β_2 are obtained under both symmetric and asymmetric loss functions. Specifically, the squared error loss (SEL), the LINEX loss, and the generalized entropy loss (GEL) function are considered. The choice of loss function plays a central role in Bayesian estimation because it determines how estimation errors are penalized and, consequently, how posterior information is summarized into a point estimator. The SEL is appropriate when overestimation and underestimation are equally undesirable. The LINEX loss is suitable when the cost of overestimation differs from that of underestimation, which is common in reliability and risk-sensitive decision problems. The GEL is useful when multiplicative or relative estimation errors are of primary concern. For this reason, considering several loss functions provides a more comprehensive Bayesian analysis and allows the proposed methodology to accommodate a wider range of practical decision-making settings.

It is assumed that the parameters α, β_1, and β_2 are a priori independent and follow gamma prior distributions with shape parameters a_i and scale parameters b_i for $i = 1, 2, 3$, respectively. Accordingly, the joint prior density function of $\boldsymbol{\theta} = (\alpha, \beta_1, \beta_2)$ is given by

$$\pi(\alpha, \beta_1, \beta_2) \propto \alpha^{a_1-1}\beta_1^{a_2-1}\beta_2^{a_3-1}\exp\left(-b_1\alpha - b_2\beta_1 - b_3\beta_2\right), \quad \alpha, \beta_1, \beta_2 > 0, \tag{4.1}$$

where $a_i > 0$ and $b_i > 0$, for $i = 1, 2, 3$.

The choice of gamma priors is motivated by mathematical convenience, conjugacy-like behavior, and compatibility with positive parameters, where the gamma family provides a natural, flexible, and

mathematically convenient prior specification on the positive real line. Moreover, gamma priors are widely used in lifetime and reliability analysis and facilitate stable posterior computation. We also mention that alternative positive-support priors, such as log-normal or other weakly informative priors, could be considered; however, the gamma choice provides a reasonable balance between interpretability and computational feasibility in the present setting.

Combining the likelihood function in Eq (3.1) with the joint prior density, the joint posterior density function of $(\alpha, \beta_1, \beta_2)$ is obtained as

$$\begin{aligned}
\pi^*(\alpha,\beta_1,\beta_2 \mid \mathbf{t}) &\propto L(\alpha,\beta_1,\beta_2 \mid \mathbf{t})\,\pi(\alpha,\beta_1,\beta_2) \\
&\propto \alpha^{4m+a_1-1}\beta_1^{m_1+a_2-1}\beta_2^{m_2+a_3-1}(1+\alpha)^{-2m} \\
&\quad \times \exp(-b_1\alpha - b_2\beta_1 - b_3\beta_2) \\
&\quad \times \prod_{i=1}^{m}\Bigg[\left(\frac{e^{\beta_1 t_i}(\alpha+e^{\beta_1 t_i}+1)(\alpha+e^{\beta_2 t_i})}{(\alpha+1)^2(\alpha+e^{\beta_1 t_i}-1)^3(\alpha+e^{\beta_2 t_i}-1)^2}\right)^{I(\delta_i=1)} \\
&\quad \times \left(\frac{e^{\beta_2 t_i}(\alpha+e^{\beta_2 t_i})(\alpha+e^{\beta_2 t_i}+1)}{(\alpha+1)^2(\alpha+e^{\beta_1 t_i}-1)^2(\alpha+e^{\beta_2 t_i}-1)^3}\right)^{I(\delta_i=2)} \\
&\quad \times \left(\frac{(\alpha+e^{\beta_1 t_i})(\alpha+e^{\beta_2 t_i})}{(\alpha+1)^2(\alpha+e^{\beta_1 t_i}-1)^2(\alpha+e^{\beta_2 t_i}-1)^2}\right)^{R_i}\Bigg].
\end{aligned} \tag{4.2}$$

Due to the complicated form of the posterior density, closed-form expressions for the Bayes estimators are not available. Therefore, all Bayesian estimators are computed numerically using posterior expectations or quantiles.

4.1. Bayesian estimation under squared error loss function

Under the SEL function, the Bayes estimator of a parameter θ is given by its posterior mean as follows

$$\widehat{\theta}_{\text{SEL}} = E(\theta \mid \mathbf{t}). \tag{4.3}$$

Hence, the Bayes estimators of α, β_1, and β_2 under SEL are given by

$$\widehat{\alpha}_{\text{SEL}} = E(\alpha \mid \mathbf{t}), \tag{4.4}$$

$$\widehat{\beta}_{1,\text{SEL}} = E(\beta_1 \mid \mathbf{t}), \tag{4.5}$$

$$\widehat{\beta}_{2,\text{SEL}} = E(\beta_2 \mid \mathbf{t}). \tag{4.6}$$

4.2. Bayesian estimation under LINEX loss function

The LINEX loss function is defined as

$$L(\Delta) = c\left(e^{k\Delta} - k\Delta - 1\right), \qquad k \neq 0, \tag{4.7}$$

where $\Delta = \widehat{\theta} - \theta$.

Under the LINEX loss function, the Bayes estimator of θ is given by

$$\widehat{\theta}_{\text{LINEX}} = -\frac{1}{k}\log\left[E\left(e^{-k\theta} \mid \mathbf{t}\right)\right]. \tag{4.8}$$

Thus, the Bayes estimators of α, β_1, and β_2 under LINEX loss are obtained by replacing θ accordingly.

4.3. Bayesian estimation under generalized entropy loss function

The GEL function is defined as

$$L(\widehat{\theta},\theta) = \left(\frac{\widehat{\theta}}{\theta}\right)^{q} - q\log\left(\frac{\widehat{\theta}}{\theta}\right) - 1, \qquad q \neq 0. \tag{4.9}$$

Under GEL, the Bayes estimator of θ is given by

$$\widehat{\theta}_{\mathrm{GEL}} = \left[E\left(\theta^{-q} \mid \mathbf{t}\right)\right]^{-1/q}. \tag{4.10}$$

All posterior expectations and quantiles required for computing the Bayesian estimators are evaluated numerically. The performance of the proposed Bayesian estimators is examined through simulation studies and real data analysis in the subsequent sections.

4.4. Metropolis-Hastings approximation for Bayesian estimates

Due to the intractable form of the joint posterior density $\pi^*(\alpha,\beta_1,\beta_2 \mid \mathbf{t})$, closed-form expressions for the Bayesian estimators are not available. Consequently, Markov chain Monte Carlo (MCMC) techniques are employed to generate samples from the posterior distribution.

In particular, a Metropolis-Hastings (MH) algorithm is implemented to simulate a three-dimensional Markov chain with stationary distribution $\pi^*(\alpha,\beta_1,\beta_2 \mid \mathbf{t})$. The generated posterior samples are then used to compute the Bayesian estimators under different loss functions as well as credible intervals for the model parameters.

Algorithm 1 Metropolis-Hastings algorithm for (α,β_1,β_2)

1: Choose initial values $(\alpha^{(0)},\beta_1^{(0)},\beta_2^{(0)})$ and set the number of iterations N.
2: Specify proposal distributions $q_1(\alpha^* \mid \alpha^{(i-1)})$, $q_2(\beta_1^* \mid \beta_1^{(i-1)})$, $q_3(\beta_2^* \mid \beta_2^{(i-1)})$.
3: **For** ($i = 1$ to N)
4: Generate proposals: $\alpha^* \sim q_1(\cdot \mid \alpha^{(i-1)})$, $\beta_1^* \sim q_2(\cdot \mid \beta_1^{(i-1)})$, $\beta_2^* \sim q_3(\cdot \mid \beta_2^{(i-1)})$.
5: Compute the acceptance probability $\rho = \min\left\{1, \frac{\pi^*(\alpha^*,\beta_1^*,\beta_2^*|\mathbf{t})\, q_1(\alpha^{(i-1)}|\alpha^*)\, q_2(\beta_1^{(i-1)}|\beta_1^*)\, q_3(\beta_2^{(i-1)}|\beta_2^*)}{\pi^*(\alpha^{(i-1)},\beta_1^{(i-1)},\beta_2^{(i-1)}|\mathbf{t})\, q_1(\alpha^*|\alpha^{(i-1)})\, q_2(\beta_1^*|\beta_1^{(i-1)})\, q_3(\beta_2^*|\beta_2^{(i-1)})}\right\}$.
6: Generate $u \sim$ Uniform(0, 1).
7: **If** $u \leq \rho$ **Then**
8: Set $(\alpha^{(i)},\beta_1^{(i)},\beta_2^{(i)}) = (\alpha^*,\beta_1^*,\beta_2^*)$.
9: **Else**
10: Set $(\alpha^{(i)},\beta_1^{(i)},\beta_2^{(i)}) = (\alpha^{(i-1)},\beta_1^{(i-1)},\beta_2^{(i-1)})$.
11: **End If**
12: **End For**
13: Discard the first B samples as burn-in.
14: Use the remaining samples to compute Bayesian estimators and credible intervals.

In Algorithm 1, the proposal distributions q_1–q_3 are assumed to be independent log-normal random-walk distributions centered at the current parameter values, with tuning variances chosen to ensure adequate acceptance rates; see [5, 6]. Log-normal random-walk proposal distributions were chosen because all parameters are strictly positive, and the log-normal form naturally preserves positivity while

allowing flexible local exploration of the posterior distribution. This choice is common in Bayesian lifetime modeling and was found to provide stable acceptance behavior in our implementation.

Let $g(\alpha,\beta_1,\beta_2)$ be a function of the model parameters. The BEs of g can be approximated using MCMC-generated samples $\left(\alpha^{(i)},\beta_1^{(i)},\beta_2^{(i)}\right)$ for $i = B+1, B+2, \ldots, N$, where B denotes the burn-in period. These approximations are computed under the SEL, LINEX, and GEL loss functions as follows:

$$\hat{g}(\alpha,\beta_1,\beta_2)_{SEL} = \frac{1}{N-B}\sum_{i=B+1}^{N} g(\alpha^{(i)},\beta_1^{(i)},\beta_2^{(i)}), \tag{4.11}$$

$$\hat{g}(\alpha,\beta_1,\beta_2)_{LINEX} = \frac{-1}{k}\log\left[\frac{1}{N-B}\sum_{i=B+1}^{N}\exp\{k\, g(\alpha^{(i)},\beta_1^{(i)},\beta_2^{(i)})\}\right], \tag{4.12}$$

and

$$\hat{g}(\alpha,\beta_1,\beta_2)_{GEL} = \left[\frac{1}{N-B}\sum_{i=B+1}^{N}[g(\alpha^{(i)},\beta_1^{(i)},\beta_2^{(i)})]^{-q}\right]^{-1/q}. \tag{4.13}$$

4.5. Bayesian credible intervals

The $100(1-\gamma)\%$ Bayesian credible CI for a parameter θ, where θ is α, β_1, or β_2 is given by

$$\int_{L}^{U}\pi^*(\theta|\underline{\mathbf{t}})d\theta = 1-\gamma, \tag{4.14}$$

where L and U denote the lower and upper bounds of the credible interval, respectively.

Due to the analytical complexity of the integral in (4.14), the MCMC approximation for the credible intervals is employed, utilizing the $(N-B)$ produced parameter values. By arranging the produced values of the parameters in ascending order as follows: $\left(\alpha^{(B+1)},\alpha^{(B+2)},\alpha^{(B+3)},...,\alpha^{(N)}\right)$, $\left(\beta_1^{(B+1)},\beta_1^{(B+2)},\beta_1^{(B+3)},...,\beta_1^{(N)}\right)$, and $\left(\beta_2^{(B+1)},\beta_2^{(B+2)},\beta_2^{(B+3)},...,\beta_2^{(N)}\right)$. Then, the $100(1-\gamma)\%$ are given as follows:

$$(\alpha^{(w_1)},\alpha^{(w_2)}), \qquad (\beta_1^{(w_1)},\beta_1^{(w_2)}), \qquad \text{and} \qquad (\beta_2^{(w_1)},\beta_2^{(w_2)}),$$

where $w_1 = ((N-B)\gamma/2)$, and $w_2 = ((N-B)(1-\gamma/2))$.

4.6. Tierney-Kadane approximation for Bayesian estimates

Bayesian inference provides a coherent and systematic framework for statistical analysis by integrating prior knowledge with information derived from observed data. In many applied settings, posterior characteristics such as means, variances, and other Bayes estimators do not admit closed-form expressions, as they are typically defined through ratios of high-dimensional integrals. This challenge becomes particularly acute in models characterized by complex likelihood functions or multiple unknown parameters. As a result, analytical approximation techniques play a central role in practical Bayesian computation.

Laplace-type approximation methods yield accurate asymptotic evaluations of posterior quantities by exploiting the local behavior of the posterior density around its mode. Within this class of

techniques, the Tierney-Kadane approximation [27] represents a notable refinement, as it is specifically designed to approximate ratios of integrals that commonly arise in Bayesian point estimation. Due to its favorable balance between accuracy and computational efficiency, the Tierney-Kadane method has been extensively employed in contemporary statistical applications, including reliability analysis, lifetime data modeling, and competing risks inference.

Let $\mathbf{t}$ denote the observed data, and let $\boldsymbol{\theta} = (\alpha, \beta_1, \beta_2)$ be a vector of unknown parameters with prior density $\pi(\boldsymbol{\theta})$. Given the likelihood function $L(\boldsymbol{\theta} \mid \mathbf{t})$, the posterior density is defined, up to a normalizing constant, as

$$\pi^*(\boldsymbol{\theta} \mid \mathbf{t}) \propto L(\boldsymbol{\theta} \mid \mathbf{t})\, \pi(\boldsymbol{\theta}).$$

For any real-valued function $g(\boldsymbol{\theta})$, the corresponding posterior expectation can be expressed as

$$\mathbb{E}[g(\boldsymbol{\theta}) \mid \mathbf{t}] = \frac{\int g(\boldsymbol{\theta}) \exp\{r(\boldsymbol{\theta})\}\, d\boldsymbol{\theta}}{\int \exp\{r(\boldsymbol{\theta})\}\, d\boldsymbol{\theta}}, \tag{4.15}$$

where $r(\boldsymbol{\theta}) = \log L(\boldsymbol{\theta} \mid \mathbf{t}) + \log \pi(\boldsymbol{\theta})$ denotes the log-posterior kernel.

Under the Tierney-Kadane framework, the scaled objective function is defined as follows:

$$\psi(\alpha, \beta_1, \beta_2) = \frac{1}{n} \left\{ \log L(\alpha, \beta_1, \beta_2 \mid \mathbf{t}) + \log \pi(\alpha, \beta_1, \beta_2) \right\},$$

together with its g-modified version,

$$\psi^g(\alpha, \beta_1, \beta_2) = \psi(\alpha, \beta_1, \beta_2) + \frac{1}{n} \log g(\alpha, \beta_1, \beta_2).$$

Let $(\hat{\alpha}_\psi, \hat{\beta}_{1\psi}, \hat{\beta}_{2\psi})$ and $(\hat{\alpha}_{\psi^g}, \hat{\beta}_{1\psi^g}, \hat{\beta}_{2\psi^g})$ be the maximizers of ψ and ψ^g, respectively; then, the corresponding Tierney-Kadane approximation to the posterior expectation in (4.15) is expressed as

$$\mathbb{E}[g(\boldsymbol{\theta}) \mid \mathbf{t}] \approx \left(\frac{|\Omega^g|}{|\Omega|} \right)^{1/2} \exp\left\{ n \left[\psi^g(\hat{\alpha}_{\psi^g}, \hat{\beta}_{1\psi^g}, \hat{\beta}_{2\psi^g}) - \psi(\hat{\alpha}_\psi, \hat{\beta}_{1\psi}, \hat{\beta}_{2\psi}) \right] \right\}, \tag{4.16}$$

where $|\Omega|$ and $|\Omega^g|$ denote the determinants of the matrices obtained by inverting the negative Hessians of ψ and ψ^g, respectively, each evaluated at its associated maximizer.

By appropriately specifying $g(\boldsymbol{\theta})$ under squared error loss, the Tierney-Kadane approximation to the Bayes estimator of α is obtained by taking $g(\alpha, \beta_1, \beta_2) = \alpha$.

$$\tilde{\alpha}_{\mathrm{TK}} = \left(\frac{|\Omega^\alpha|}{|\Omega|} \right)^{1/2} \exp\left\{ n \left[\psi^\alpha(\hat{\alpha}_{\psi^\alpha}, \hat{\beta}_{1\psi^\alpha}, \hat{\beta}_{2\psi^\alpha}) - \psi(\hat{\alpha}_\psi, \hat{\beta}_{1\psi}, \hat{\beta}_{2\psi}) \right] \right\}.$$

Likewise, the Tierney-Kadane Bayes estimators for β_1 and β_2 are expressed, respectively, as

$$\tilde{\beta}_{1,\mathrm{TK}} = \left(\frac{|\Omega^{\beta_1}|}{|\Omega|} \right)^{1/2} \exp\left\{ n \left[\psi^{\beta_1}(\hat{\alpha}_{\psi^{\beta_1}}, \hat{\beta}_{1\psi^{\beta_1}}, \hat{\beta}_{2\psi^{\beta_1}}) - \psi(\hat{\alpha}_\psi, \hat{\beta}_{1\psi}, \hat{\beta}_{2\psi}) \right] \right\}$$

and

$$\tilde{\beta}_{2,\mathrm{TK}} = \left(\frac{|\Omega^{\beta_2}|}{|\Omega|} \right)^{1/2} \exp\left\{ n \left[\psi^{\beta_2}(\hat{\alpha}_{\psi^{\beta_2}}, \hat{\beta}_{1\psi^{\beta_2}}, \hat{\beta}_{2\psi^{\beta_2}}) - \psi(\hat{\alpha}_\psi, \hat{\beta}_{1\psi}, \hat{\beta}_{2\psi}) \right] \right\}.$$

5. Simulation study and numerical results

During this section, a comprehensive simulation study is designed to assess and compare the finite-sample performance of classical and Bayesian estimation procedures for the parameters of the Gompertz-Lindley competing risks model under progressive Type-II censoring. The primary objective is to evaluate the accuracy and stability of the estimators of the model parameters α, β_1, and β_2 under various censoring schemes and sample sizes. One thousand independent samples are generated from the GLD under a competing-risks framework with two latent causes of failure based on the following real values of parameters $(\alpha, \beta_1, \beta_2) = (1.1, 0.5, 0.8)$. These parameter values represent a moderate and practically meaningful configuration for the Gompertz-Lindley competing-risks model, producing realistic lifetime behavior and distinguishable cause-specific effects. The progressive Type-II samples are generated with different sample sizes n and effective number of failures m as follows: $(n, m) = (30, 20), (40, 30), (60, 40)$, and $(70, 50)$. We must note that multiple sample sizes were considered to assess the performance of the estimators under both small and moderate sample conditions. This design allows for evaluating the robustness of the proposed methods under different practical scenarios. As we can remove reliable units during the test according to progressive Type-II censoring, the following three censoring schemes are considered:

(1) Scheme 1: $R_1 = n - m$ and $R_i = 0,\ i = 2, ..., m$.
(2) Scheme 2: $R_i = 1,\ i = 1, 2, ..., n - m$; otherwise, $R_i = 0$.
(3) Scheme 3: $R_i = 0,\ i = 1, 2, ..., m - 1$, and $R_m = n - m$.

The choice of these three censoring schemes directly affects estimation accuracy. Early censoring reduces available information and increases variability, whereas late censoring retains more observations and yields more stable and accurate estimates. Balanced schemes provide a compromise between efficiency and cost.

In particular, Scheme 1 (early censoring) leads to limited information, Scheme 2 (distributed censoring) tends to produce higher variability, and Scheme 3 (late censoring) provides the most accurate estimates. From a practical perspective, Scheme 1 may be preferred when cost reduction is the main objective, Scheme 3 is recommended for achieving higher estimation accuracy, and Scheme 2 offers a balanced alternative.

Bayesian point estimates are computed under different loss functions, including the SEL, LINEX loss, and GE loss, to examine the robustness of Bayesian inference to asymmetric loss structures. Regarding the LINEX loss function, it has been excuted with hyperparameters set as $k = -0.5$ and 0.5, and the hyperparameters of the GEL function is chosen as $q = -1.5$, and 1.5. Also, the Bayesian estimates are approximated using the Tierney-Kadane (T-K) approximation method.

For the prior distributions of the model parameters, informative gamma priors are assumed. Specifically, the shape parameter α is assigned a gamma prior with hyperparameters (a_1, b_1), whereas the scale parameters β_1 and β_2 are independently assigned gamma priors with hyperparameters (a_2, b_2) and (a_3, b_3), respectively. The values of these hyperparameters are determined using a data-driven approach based on preliminary simulations, as described below.

(1) Generate l independent samples from the Gompertz-Lindley competing risks model under the specified progressive censoring scheme.

(2) For each generated sample, compute the maximum likelihood estimates

$$(\hat{\alpha}^j, \hat{\beta}_1^j, \hat{\beta}_2^j), \qquad j = 1, 2, \ldots, l.$$

(3) Calculate the sample mean and variance of the estimates for each parameter $\Theta \in \{\alpha, \beta_1, \beta_2\}$ as $\bar{\Theta} = l^{-1} \sum_{j=1}^{l} \hat{\Theta}^j$, $S_{\Theta}^2 = (l-1)^{-1} \sum_{j=1}^{l} \left(\hat{\Theta}^j - \bar{\Theta}\right)^2$.

(4) Assume that the prior distribution of Θ follows a gamma distribution with density $\pi(\Theta) \propto \Theta^{a-1} \exp(-b\Theta)$, which has mean a/b and variance a/b^2. The corresponding hyperparameters (a, b) are obtained by solving the following system of equations:

$$\begin{aligned} \frac{a}{b} &= \bar{\Theta}, \\ \frac{a}{b^2} &= S_{\Theta}^2. \end{aligned}$$

Also, consider the MCMC method in Algorithm 1, where the number of MCMC iterations is 2000 with burn in period 500.

The estimators are evaluated using standard accuracy criteria. The following metrics are calculated for each parameter: average estimate (AE), relative absolute bias (RAB), and mean squared error (MSE). The criteria RAB and MSE are chosen because they jointly summarize estimator accuracy, bias, and stability, and they are widely used in simulation studies for censored competing-risks models.

Tables 1–3 provide a summary of the numerical results, reporting the AE, RAB, and MSE values for all estimators across various sample sizes and censoring techniques. The average length (AL) and coverage probability (CP) of the asymptotic confidence intervals (ACI) and Bayesian credible intervals (CCI) for the parameters α, β_1, and β_2 under various sample sizes and censoring strategies are compared in Table 4.

Table 1. AE, RAB, and MSE for different estimates of α.

n	m	Sch		MLE	T-K	SEL	LINEX1	LINEX2	GE1	GE2
30	20	1	AE	1.39168	1.21162	1.32215	1.26651	1.39171	1.13209	1.36445
			RAB	0.64089	0.18397	0.24210	0.20454	0.29319	0.15856	0.26952
			MSE	0.76859	0.06758	0.11500	0.08257	0.16795	0.04756	0.14052
		2	AE	1.08070	1.16994	1.25243	1.20822	1.30553	1.09007	1.28789
			RAB	0.76096	0.15648	0.19880	0.17457	0.23266	0.15942	0.21723
			MSE	0.90356	0.05194	0.08702	0.06729	0.11812	0.05478	0.10222
		3	AE	1.33867	1.20609	1.30828	1.25655	1.37196	1.12933	1.34790
			RAB	0.63577	0.17854	0.23188	0.19881	0.27827	0.16051	0.25731
			MSE	0.74654	0.06336	0.10890	0.07996	0.15505	0.04847	0.13153
40	30	1	AE	1.27665	1.20385	1.26946	1.22990	1.31599	1.12704	1.30028
			RAB	0.52344	0.15428	0.21210	0.18531	0.24639	0.14566	0.23263
			MSE	0.47566	0.04638	0.09252	0.07359	0.12099	0.04958	0.10763
		2	AE	0.77116	1.11451	1.19577	1.16245	1.23378	1.06206	1.22391
			RAB	0.56859	0.10875	0.13884	0.12310	0.16076	0.11687	0.15247
			MSE	0.52708	0.02116	0.03637	0.02839	0.04883	0.02845	0.04367
		3	AE	1.02290	1.12640	1.20791	1.17294	1.24793	1.07242	1.23699
			RAB	0.42142	0.12394	0.15075	0.13351	0.17438	0.11759	0.16533
			MSE	0.31343	0.02693	0.04180	0.03210	0.05652	0.02443	0.05053
60	40	1	AE	1.31662	1.20406	1.27256	1.23893	1.31015	1.14608	1.29892
			RAB	0.51859	0.14218	0.18609	0.16433	0.21213	0.13358	0.20236
			MSE	0.46869	0.04674	0.07128	0.05649	0.09132	0.03610	0.08298
		2	AE	1.58749	1.13660	1.20019	1.17137	1.23232	1.08443	1.22436
			RAB	0.98369	0.12345	0.17256	0.15972	0.18983	0.15275	0.18233
			MSE	1.87169	0.03042	0.06454	0.05580	0.07705	0.05568	0.07111
		3	AE	1.49743	1.17770	1.25851	1.22684	1.29407	1.14134	1.28333
			RAB	0.65588	0.16088	0.19728	0.17894	0.22006	0.15506	0.21076
			MSE	0.97243	0.05075	0.07939	0.06481	0.09917	0.04586	0.09039
70	50	1	AE	1.23208	1.15101	1.21376	1.18609	1.24428	1.10606	1.23640
			RAB	0.44702	0.12470	0.15345	0.14115	0.16982	0.12775	0.16340
			MSE	0.38876	0.03470	0.05256	0.04340	0.06496	0.03336	0.05976
		2	AE	1.01884	1.11135	1.15413	1.12930	1.18157	1.05584	1.17551
			RAB	0.56644	0.10016	0.17993	0.16804	0.19466	0.15677	0.18859
			MSE	0.53901	0.01795	0.08367	0.07762	0.09215	0.07315	0.08772
		3	AE	1.38389	1.15663	1.22339	1.19637	1.25328	1.11932	1.24522
			RAB	0.54952	0.14156	0.16750	0.15372	0.18491	0.13922	0.17801
			MSE	0.66444	0.03977	0.06032	0.05020	0.07407	0.03842	0.06804

Table 2. AE, RAB, and MSE for different estimates of β_1.

n	m	Sch		MLE	T-K	SEL	LINEX1	LINEX2	GE1	GE2
30	20	1	AE	0.58438	0.50137	0.53366	0.52582	0.54181	0.45960	0.54812
			RAB	0.61680	0.13237	0.15186	0.14527	0.15970	0.15152	0.16327
			MSE	0.14688	0.00683	0.00908	0.00830	0.01004	0.00873	0.01045
		2	AE	0.47847	0.50342	0.52982	0.52159	0.53845	0.45201	0.54527
			RAB	0.77612	0.13883	0.15374	0.14808	0.16069	0.16787	0.16273
			MSE	0.19715	0.00717	0.00950	0.00877	0.01041	0.01122	0.01070
		3	AE	0.56533	0.50071	0.53082	0.52311	0.53886	0.45759	0.54514
			RAB	0.61338	0.13376	0.15339	0.14704	0.16064	0.15572	0.16356
			MSE	0.14169	0.00716	0.00946	0.00872	0.01036	0.00945	0.01072
40	30	1	AE	0.55122	0.50052	0.52286	0.51638	0.52956	0.46088	0.53495
			RAB	0.55488	0.14813	0.17422	0.16901	0.18049	0.17004	0.18270
			MSE	0.10780	0.00863	0.01300	0.01239	0.01375	0.01274	0.01398
		2	AE	0.33494	0.48957	0.51973	0.51271	0.52703	0.45151	0.53311
			RAB	0.58432	0.12051	0.13392	0.12933	0.13944	0.15040	0.14165
			MSE	0.11305	0.00579	0.00707	0.00661	0.00766	0.00936	0.00786
		3	AE	0.44496	0.48719	0.51550	0.50908	0.52215	0.45306	0.52776
			RAB	0.43634	0.12412	0.13426	0.13053	0.13881	0.14594	0.14038
			MSE	0.06909	0.00593	0.00691	0.00652	0.00741	0.00817	0.00759
60	40	1	AE	0.54160	0.49290	0.51667	0.51102	0.52248	0.46099	0.52744
			RAB	0.49483	0.15094	0.15370	0.15116	0.15698	0.16142	0.15717
			MSE	0.09040	0.00806	0.00957	0.00914	0.01009	0.01014	0.01220
		2	AE	0.69890	0.50727	0.53143	0.52471	0.53839	0.46819	0.54401
			RAB	0.96123	0.13293	0.16449	0.15971	0.17024	0.16797	0.17181
			MSE	0.34770	0.00694	0.01189	0.01123	0.01269	0.01271	0.01289
		3	AE	0.64642	0.51085	0.54045	0.53429	0.54683	0.48396	0.55163
			RAB	0.63138	0.14268	0.16841	0.16286	0.17466	0.15402	0.17694
			MSE	0.17202	0.00816	0.01165	0.01084	0.01257	0.00921	0.01291
70	50	1	AE	0.55283	0.51077	0.53422	0.52865	0.53993	0.48245	0.54441
			RAB	0.47275	0.14561	0.16273	0.15776	0.16806	0.14853	0.16971
			MSE	0.08482	0.00804	0.00940	0.00994	0.01134	0.00854	0.01162
		2	AE	0.44900	0.49158	0.51006	0.50420	0.51614	0.45564	0.52119
			RAB	0.58362	0.11886	0.17959	0.17515	0.18481	0.18130	0.18613
			MSE	0.11493	0.00557	0.01788	0.01734	0.01852	0.01737	0.01853
		3	AE	0.60780	0.51021	0.53554	0.52999	0.54126	0.48412	0.54572
			RAB	0.53593	0.13925	0.15873	0.15392	0.16414	0.14556	0.16638
			MSE	0.12237	0.00743	0.00987	0.00924	0.01058	0.00813	0.01087

Table 3. AE, RAB, and MSE for different estimates of β_2.

n	m	Sch		MLE	T-K	SEL	LINEX1	LINEX2	GE1	GE2
30	20	1	AE	0.93703	0.80502	0.83958	0.82949	0.85000	0.77843	0.85158
			RAB	0.58023	0.07018	0.08505	0.07938	0.09194	0.07558	0.09223
			MSE	0.32485	0.00485	0.00721	0.00629	0.00839	0.00557	0.00843
		2	AE	0.77240	0.80041	0.82876	0.81795	0.83999	0.76126	0.84204
			RAB	0.76078	0.05975	0.07832	0.07314	0.08503	0.07915	0.08500
			MSE	0.47991	0.00349	0.00690	0.00631	0.00776	0.01015	0.00760
		3	AE	0.90810	0.80234	0.83515	0.82506	0.84557	0.77389	0.84719
			RAB	0.58965	0.06954	0.08450	0.07904	0.09120	0.07706	0.09147
			MSE	0.32927	0.00483	0.00772	0.00686	0.00883	0.00650	0.00886
40	30	1	AE	0.84788	0.80242	0.82016	0.81131	0.82927	0.76623	0.83083
			RAB	0.43764	0.06317	0.08140	0.07724	0.08658	0.07926	0.08688
			MSE	0.19838	0.00600	0.01153	0.01096	0.01229	0.01118	0.01232
		2	AE	0.57623	0.79846	0.83413	0.82393	0.84468	0.77014	0.84648
			RAB	0.58609	0.05738	0.07630	0.07060	0.08378	0.07347	0.08415
			MSE	0.28956	0.00332	0.00610	0.00539	0.00706	0.00815	0.00700
		3	AE	0.74757	0.79402	0.82680	0.81771	0.83615	0.77092	0.83776
			RAB	0.43830	0.07128	0.08245	0.07833	0.08766	0.07862	0.08776
			MSE	0.47844	0.00511	0.00679	0.00616	0.00763	0.00631	0.00763
60	40	1	AE	0.88835	0.81058	0.83851	0.82986	0.84738	0.78585	0.84880
			RAB	0.44527	0.07885	0.08972	0.08539	0.09465	0.08191	0.09459
			MSE	0.19189	0.00566	0.00797	0.00715	0.00897	0.00620	0.00899
		2	AE	1.07116	0.80723	0.83722	0.82720	0.84758	0.77441	0.84949
			RAB	0.87813	0.06111	0.10251	0.09711	0.10911	0.09607	0.10876
			MSE	0.70562	0.00370	0.01380	0.01304	0.01483	0.01686	0.01454
		3	AE	1.00183	0.81153	0.84683	0.83786	0.85606	0.79329	0.85738
			RAB	0.56156	0.07861	0.10030	0.09474	0.10666	0.08483	0.10675
			MSE	0.32817	0.00620	0.01001	0.00896	0.01128	0.00717	0.01127
70	50	1	AE	0.83818	0.79373	0.82226	0.81428	0.83043	0.77311	0.83194
			RAB	0.39453	0.07946	0.09592	0.09309	0.09945	0.09594	0.09919
			MSE	0.15374	0.00535	0.00771	0.00630	0.00848	0.00638	0.00843
		2	AE	0.75667	0.80364	0.82085	0.81137	0.83069	0.76495	0.83238
			RAB	0.60016	0.06000	0.13316	0.12758	0.13929	0.12111	0.13884
			MSE	0.32011	0.00352	0.03414	0.03307	0.03546	0.03218	0.03485
		3	AE	0.94546	0.81002	0.84065	0.83228	0.84924	0.78997	0.85058
			RAB	0.48609	0.07823	0.09726	0.09286	0.10232	0.08690	0.10226
			MSE	0.24454	0.00608	0.00974	0.00885	0.01081	0.00771	0.01078

Table 4. The average length (AL) and coverage probability (CP) for the ACI and CCI estimation of the parameters.

n	m	sch	Parameter	ACI-AL	ACI-CP	CCI-AL	CCI-CP
30	20	1	α	5.4170	0.9930	1.8577	1.0000
			β_1	2.2000	0.9660	0.6860	1.0000
			β_2	3.1094	0.9860	0.7849	1.0000
		2	α	9.3958	1.0000	1.6440	0.9980
			β_1	4.1775	0.9780	0.7024	0.9990
			β_2	6.2186	0.9860	0.8076	0.9990
		3	α	5.3608	0.9870	1.7920	0.9990
			β_1	2.2483	0.9660	0.6809	0.9990
			β_2	3.2302	0.9790	0.7836	0.9990
40	30	1	α	3.9404	0.9930	1.4763	1.0000
			β_1	1.7503	0.9740	0.6216	0.9990
			β_2	2.6407	0.9880	0.7473	1.0000
		2	α	6.6659	0.9900	1.4306	1.0000
			β_1	2.9849	0.9510	0.6486	1.0000
			β_2	4.7254	0.9610	0.7858	1.0000
		3	α	3.93584	0.989	1.47601	1.0000
			β_1	1.75433	0.967	0.62020	0.9990
			β_2	2.61807	0.976	0.74383	1.0000
60	40	1	α	3.8923	0.9930	1.4123	0.9960
			β_1	1.6127	0.9690	0.6053	0.9950
			β_2	2.2420	0.9670	0.7243	0.9990
		2	α	7.6504	0.9970	1.2910	0.9860
			β_1	3.3035	0.9760	0.6210	0.9920
			β_2	4.7601	0.9800	0.7648	0.9930
		3	α	3.9217	0.9950	1.3809	0.9920
			β_1	1.6499	0.9710	0.6026	0.9940
			β_2	2.3193	0.9690	0.7317	1.0000
70	50	1	α	3.4108	0.9960	1.3105	0.9940
			β_1	1.4226	0.9730	0.5718	0.9970
			β_2	1.9826	0.9650	0.7057	1.0000
		2	α	6.2150	0.9950	1.2213	0.9820
			β_1	2.6908	0.9690	0.5994	0.9860
			β_2	3.8916	0.9650	0.7411	0.9860
		3	α	3.3606	0.9980	1.2669	0.9890
			β_1	1.4470	0.9810	0.5707	0.9950
			β_2	2.0538	0.9670	0.7064	0.9990

A closer examination of Tables 1–4 provides several useful practical insights into the relative strengths and limitations of the proposed inferential procedures. The following is a detailed explanation of these points.

(1) Bayesian estimators dominate the MLE in small and moderate samples, especially under progressive censoring, because they yield much smaller RAB and MSE values for all three parameters. This is particularly clear for α, where the MLE often has substantially larger RAB and MSE than the Bayesian alternatives across all censoring schemes.
(2) The T-K estimator is especially competitive, and for β_1 and β_2, it is often the best or among the best performers in terms of MSE across nearly all sample sizes and censoring schemes.
(3) Among asymmetric-loss Bayes estimators, performance depends on the parameter and censoring scheme. For α, some asymmetric choices (notably GE1 and sometimes LINEX1) can provide improvements over SEL, especially under heavier censoring, but for β_1 and β_2, the gains over T-K are limited. This shows that asymmetric losses offer flexibility, but they do not uniformly outperform all other Bayes procedures.
(4) All estimators improve as n and m increase because both MSE and RAB decrease with larger effective sample information. This supports the consistency of the proposed inferential procedures.
(5) Censoring scheme matters: The second censoring scheme generally produces greater variability and wider intervals than the first and third schemes, especially for α, indicating that this scheme is the most challenging for inference.
(6) Bayesian credible intervals are clearly preferable to asymptotic confidence intervals in finite samples because they are substantially shorter while still maintaining coverage probabilities close to the nominal level. At the same time, the ACI intervals tend to be conservative and unnecessarily wide, especially under stronger censoring and for smaller samples.
(7) A limitation should also be acknowledged: Inference for the shape parameter α is noticeably more sensitive to censoring than inference for β_1 and β_2, as seen from the larger MSEs and longer interval lengths. Thus, although the proposed procedures work well overall, stronger censoring still affects the precision of estimating α.

6. Real data application

In this section, a heart disease dataset is introduced to illustrate the estimation methods considered in this article and to illustrate that the GLD may be a possible alternative to some popular distributions. The heart disease dataset is selected because it naturally involves competing risks, where different causes may lead to failure. This makes it suitable for illustrating the applicability of the proposed model. Similar datasets from medical survival studies or reliability experiments could also be used to further validate the robustness of the model. The methods are illustrated using an observational time-to-event dataset of $n = 20$ patients with prior heart disease. For each subject, the follow-up time (in months) and the type of failure were recorded; event codes are 1 = myocardial infarction (MI) and 2 = death from other causes (D). The observed data are the follow-up time t = (1, 1.5, 2, 3.2, 4, 4.3, 5, 6.1, 7, 7.3, 8, 8.1, 8.5, 9, 10, 10.5, 11, 12, 15, 16) and the type of failure d = (1, 1, 2, 1, 2, 2, 2, 1, 2, 1, 1, 2, 2, 2, 1, 1, 1, 2, 1, 2). This dataset was displayed in Table 1.1 in [25].

To verify the suitability of the proposed data for the GLD, the unknown parameters are estimated using the maximum likelihood method, and the results are as follows: $\hat{\alpha} = 15.3691$, $\hat{\beta}_1 = 0.2655$, and $\hat{\beta}_2 = 0.2698$ with standard errors reported in Table 5. Furthermore, the Kolmogorov–Smirnov

distance (KSD) and its corresponding p-value (KSPV) are computed to assess the goodness of fit. The estimated KSD is 0.1212, with a corresponding KSPV of 0.9942, indicating that there is no statistically significant evidence against the GLD for the data considered.

Table 5. Comparison of different competing risk models for the failure time of heart disease.

		α	β_1	β_2	AIC	BIC	HQIC	CAIC
GLD	estimates	15.3691	0.2655	0.2698	145.0893	148.0765	145.6725	146.5893
	StEr	11.2503	0.0767	0.0783				
WD	estimates	1.8558	0.081975	0.081987	145.3547	148.3419	145.9378	146.8547
	StEr	0.3379	0.04739	0.04238				
EE	estimates	26.4815	0.002056	0.002041	149.6061	152.5932	150.1892	151.1061
	StEr	6.0374	0.000389	0.000375				
EW	estimates	0.0163	0.5639	0.5674	145.3609	148.3481	145.9441	146.8609
	StEr	0.0083	0.0524	0.0515				

Figure 2 shows close agreement between the empirical and fitted CDF/PDF; the PP-plot lies near the 45° reference line, and the estimated hazard exhibits an increasing trend consistent with the Gompertz-Lindley specification. These graphical diagnostics support the adequacy of the fitted model for the observed failure times.

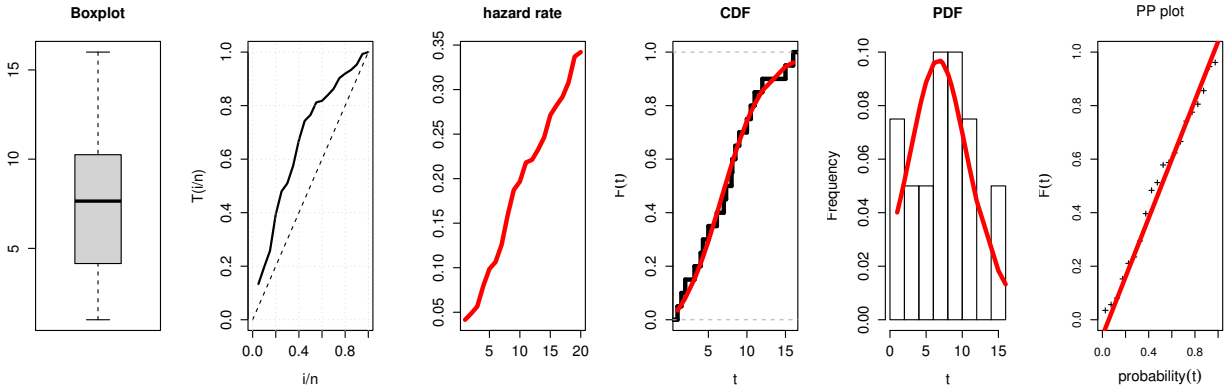

Figure 2. Fitting of failure times for the heart disease by GLD via different graphs.

To assess whether the GLD provides an adequate fit to the data, we conducted the Kolmogorov-Smirnov goodness-of-fit test and compared it with other competitive distributions, including the Weibull distribution (WD), the extension of the exponential (EE) distribution, and the exponentiated-Weibull (EW) distribution. The model selection criteria used to compare GLD with other distributions are the Akaike information criterion (AIC), Bayesian information criterion (BIC), Hannan-Quinn information criterion (HQIC), and consistent Akaike information criterion (CAIC). These criteria are defined as follows:

$$\begin{aligned} \text{AIC} &= 2k - 2\ln(\hat{L}), \\ \text{BIC} &= k\ln(n) - 2\ln(\hat{L}), \\ \text{HQIC} &= -2\ln(\hat{L}) + 2k\ln(\ln(n)), \end{aligned}$$

$$\text{CAIC} = -2\ln(\hat{L}) + k(\ln(n) + 1),$$

where $\hat{L}$ is the maximized likelihood function of the model, and k is the number of model parameters. The AIC tends to favor predictive adequacy, whereas BIC and CAIC place stronger penalties on model complexity and therefore emphasize parsimony, particularly in smaller samples. HQIC lies between these criteria in terms of penalization. Reporting all four criteria provides a more comprehensive comparison and helps ensure that model preference is not driven by a single selection rule. The values of such information criteria are reported in Table 5.

The GLD specification attains the smallest values of AIC, BIC, HQIC, and CAIC and is therefore selected as the preferred competing-risks model for these failure times. The WD, EE, and EW alternatives produce very similar AIC/HQIC figures (close to 145.36–145.94) but exceed the GLD values, whereas the EE model yields notably larger information-criterion values and is thus a poorer fit.

Figure 3 displays the profile log-likelihoods for the Gompertz-Lindley parameters; each panel shows a clear single maximum (marked) at the maximum likelihood estimate, and the sensible curvature of the profiles indicates that the parameters are well-identified. These plots support using profile-based confidence intervals for each parameter because the likelihood shapes are regular and unimodal.

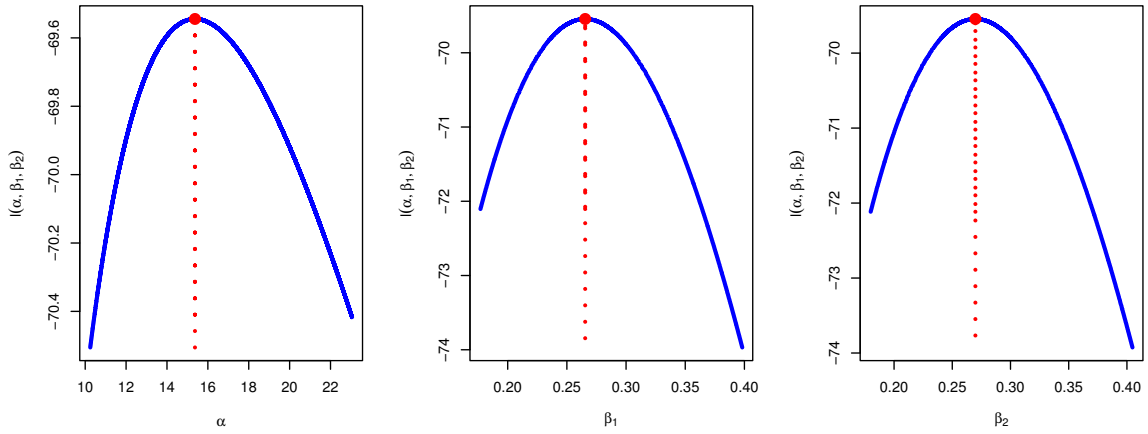

Figure 3. Likelihood profile of GLD parameters for failure times of heart disease.

Figure 4 gives contour maps of the joint log-likelihood for parameter pairs. The contours form well-defined, concentric level sets around the joint maximum, confirming a stable joint fit. The (α, β_1) and (α, β_2) plots show some elongation of the ellipses, indicating moderate parameter dependence between α and the scale parameters, whereas the (β_1, β_2) contours are closer to circular, suggesting near-orthogonality between the two β parameters. Together, the profile and contour diagnostics corroborate the reliability of the fitted GLD competing-risks model.

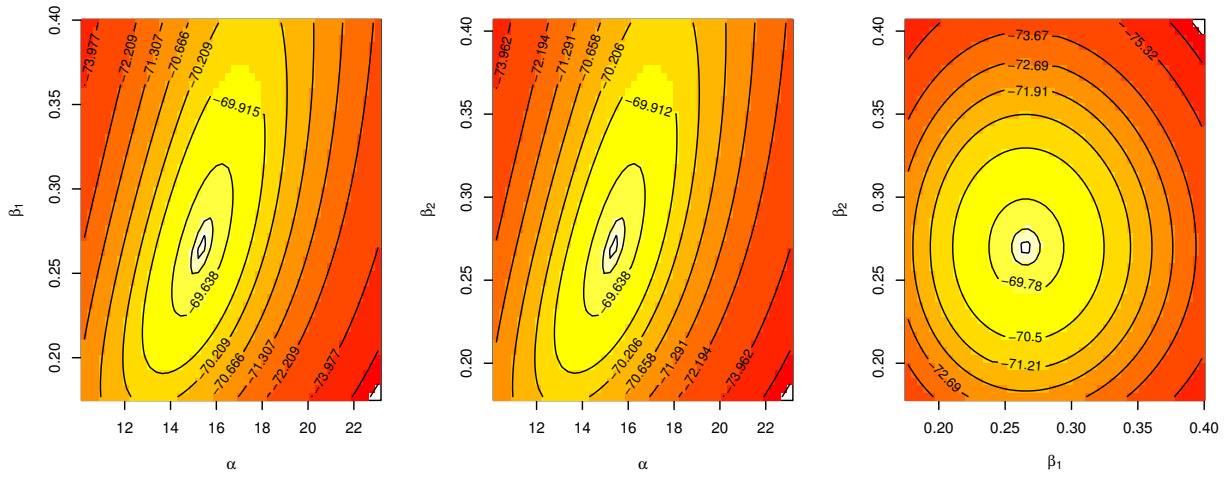

Figure 4. Contour plots of parameters GL competing risk model for the failure time of heart disease.

For the purpose of proving the efficiency of the proposed estimates for the model parameters under PC-CR, we have generated three samples from the complete data with three censoring schemes, which are shown in Table 6.

Table 6. Different samples generated from the failure time of the heart disease.

		Data														
Sample		1	2	3	4	5	6	7	8	9	10	11	12	13	14	15
	t	1	1.5	2	4.3	5	6.1	7	7.3	8.5	9	10	10.5	12	15	16
1	δ_i	1	1	2	2	2	1	2	1	2	2	1	1	2	1	2
	R_i	2	1	2	0	0	0	0	0	0	0	0	0	0	0	0
	t	1	1.5	2	3.2	4	4.3	6.1	7	8	9	10	10.5	11	12	15
2	δ_i	1	1	2	1	2	2	1	2	1	2	1	1	1	2	1
	R_i	0	3	0	0	2	0	0	0	0	0	0	0	0	0	0
	t	1	1.5	2	4.3	5	6.1	7	7.3	8.5	9	10	11	12	15	16
3	δ_i	1	1	2	2	2	1	2	1	2	2	1	1	2	1	2
	R_i	0	4	1	0	0	0	0	0	0	0	0	0	0	0	0

The estimation outcomes for α, β_1, and β_2 under three progressive censoring schemes are detailed in Tables 7 (point estimates) and 8 (interval estimates). A key finding is the elevated shape parameter α under Sample 1 across all methods, signaling stronger censoring-induced stress. Samples 2 and 3 produce lower and more similar α values. The scale parameters β_1 and β_2, however, remain stable and small regardless of scheme or estimation technique. Methodological dependability is supported by the agreement between classical (MLE, T-K) point estimates and Bayesian approaches (SEL, LINEX, GE).

Table 7. Estimated values based on progressive Type-II censoring for different schemes.

Sample		MLE	SEL	T-K	LINEX1	LINEX2	GE1	GE2
	α	14.8426	15.9590	16.4570	22.3219	12.4234	16.2939	14.3184
1	β_1	0.2619	0.2639	0.2631	0.2642	0.2637	0.2650	0.2587
	β_2	0.2395	0.2425	0.2451	0.2427	0.2422	0.2435	0.2371
	α	14.9324	15.5330	16.6360	22.6386	12.3102	15.8201	14.0962
2	β_1	0.2442	0.2431	0.2490	0.2434	0.2428	0.2443	0.2370
	β_2	0.2914	0.2929	0.2951	0.2932	0.2926	0.2940	0.2877
	α	14.9477	15.8082	16.6190	22.2744	12.2347	16.1267	14.1887
3	β_1	0.2611	0.2616	0.2644	0.2618	0.2613	0.2626	0.2567
	β_2	0.2387	0.2416	0.2423	0.2419	0.2414	0.2426	0.2365

Table 8. The asymptotic and credible interval estimation for the parameters based on the real data.

		MLE			Bayes		
Sample		ACI-L	ACI-U	L-ACI	CCI-L	CCI-U	L-CCI
	α	3.0167	38.4945	35.4779	7.9906	25.1936	17.2030
1	β_1	0.1789	0.4277	0.2488	0.2003	0.3295	0.1292
	β_2	0.1595	0.3995	0.2399	0.1826	0.3071	0.1244
	α	2.9462	26.9185	23.9722	7.5112	23.6030	16.0919
2	β_1	0.1556	0.3327	0.1771	0.1770	0.3072	0.1302
	β_2	0.2031	0.3796	0.1764	0.2247	0.3598	0.1351
	α	3.0494	26.8459	23.7965	8.1427	25.0666	16.9240
3	β_1	0.1786	0.3436	0.1649	0.2007	0.3256	0.1249
	β_2	0.1593	0.3181	0.1587	0.1801	0.3029	0.1228

Bayesian credible intervals are frequently narrower than asymptotic confidence intervals, especially for α in Samples 2 and 3, according to interval analysis (Table 8), indicating greater posterior concentration. Sample 1 has the broadest intervals for α, reflecting its larger point-estimate dispersion. High estimation precision is indicated by the constantly tight intervals for β_1 and β_2. All things considered, the findings show that Sample 1 introduces more shape-parameter uncertainty, but Samples 2 and 3 offer more consistent estimates, with Bayesian interval estimation producing marginally more effective uncertainty bounds.

To ensure the convergence of the MCMC chains, the Gelman-Rubin diagnostic was applied using two independent chains with a total of 10,000 iterations and a burn-in period of 500. The calculated potential scale reduction factor (PSRF) for all estimated parameters (α, β_1, and β_2) was very close to 1.00 (ranging from 1.01 to 1.04), with a multivariate PSRF of 1.00. These results strictly satisfy the convergence criteria (PSRF ¡ 1.1), indicating that the chains have successfully converged to the posterior distribution and the sampling is reliable. In addition to the Gelman-Rubin diagnostic, the convergence of the MCMC chains was further verified using Geweke's diagnostic and the effective sample size (ESS). The Geweke Z-scores for the three parameters α, β_1, and β_2 are 0.58, -1.16, and 1.47, respectively, that fall within the interval $[-1.96, 1.96]$, confirming that the chains reach

stationarity. Furthermore, the ESS analysis shows that the number of independent samples is sufficient for posterior inference, with ESS values ranging from 138.5 to 794.0 across parameters. These combined diagnostics ensure the reliability and stability of the MCMC estimation. Table 9 displays a summary of the convergence criterion (PSRF, Geweke, and ESS) for the three parameters.

Table 9. Summary of the convergence criteria (PSRF, Geweke, and ESS) for the three parameters.

Sample	Parameter	Gelman-Rubin (PSRF)	Geweke (Z-score)	ESS	Status
1	α	1.04	0.5808	138.5	Converged
	β_1	1.01	-1.1600	794.0	Converged
	β_2	1.01	1.4736	650.6	Converged
2	α	1.01	-0.85567	171.6	Converged
	β_1	1.01	0.07409	636.1	Converged
	β_2	1.00	-0.83348	757.1	Converged
3	α	1.00	-0.08778	149.7	Converged
	β_1	1.01	-1.74455	781.9	Converged
	β_2	1.00	-0.48843	669.6	Converged

The MCMC chains for α, β_1, and β_2 oscillate around very stable mean levels without displaying long-term trends or drift, according to the trace plots displayed in Figures 5–7. This behavior indicates that the chains exhibit appropriate mixing and have arrived at the stationary region of the posterior distribution.

For each of the three parameters, the accompanying posterior density plots show unimodal and clearly defined marginal posterior distributions, suggesting that the MCMC sampling yields accurate posterior estimates. Overall, the findings imply that Samples 1–3 produce posterior samples that are adequately informative for Bayesian inference.

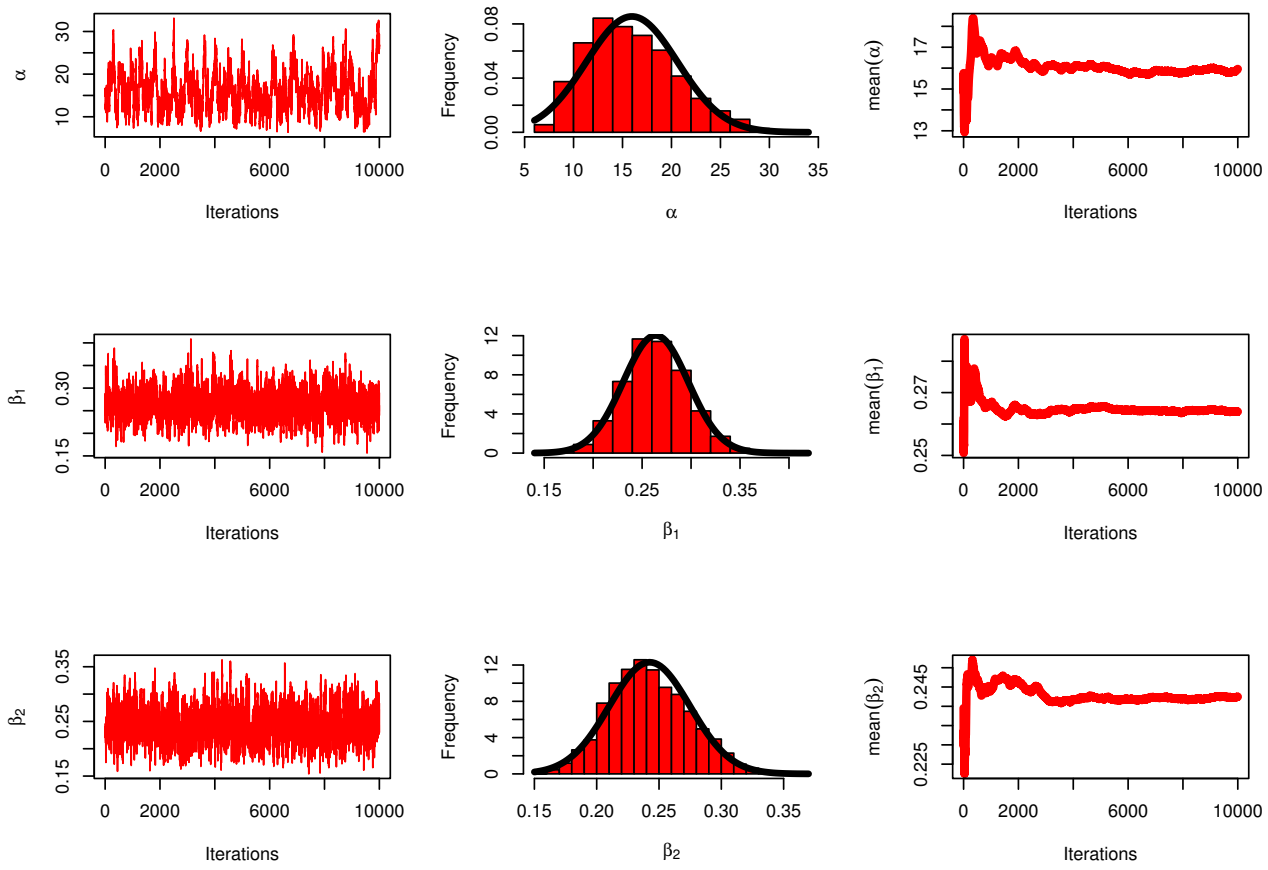

Figure 5. Trace plots and posterior density estimates of the parameters α, β_1, and β_2 obtained under Sample 1 of the real data.

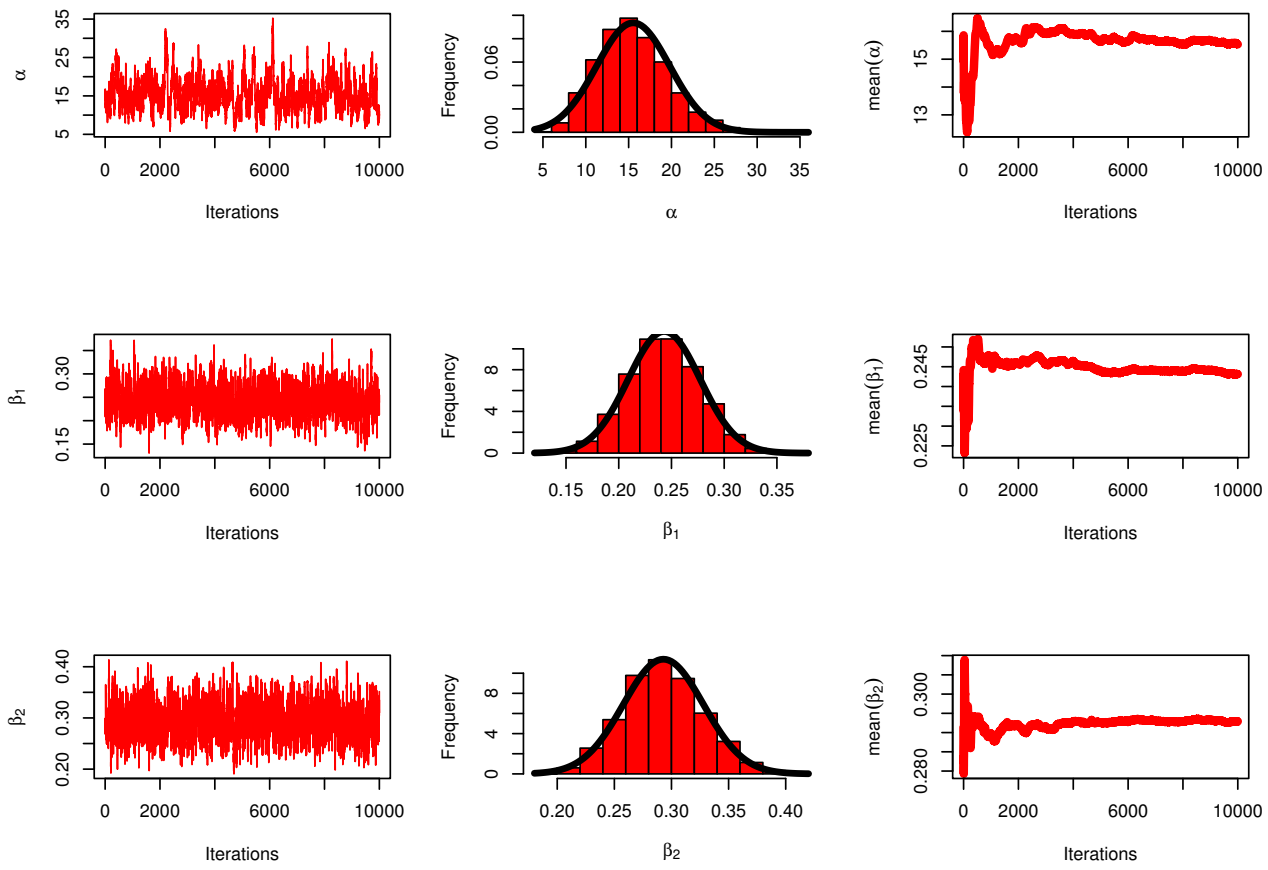

Figure 6. Trace plots and posterior density estimates of the parameters α, β_1, and β_2 obtained under Sample 2 of real data.

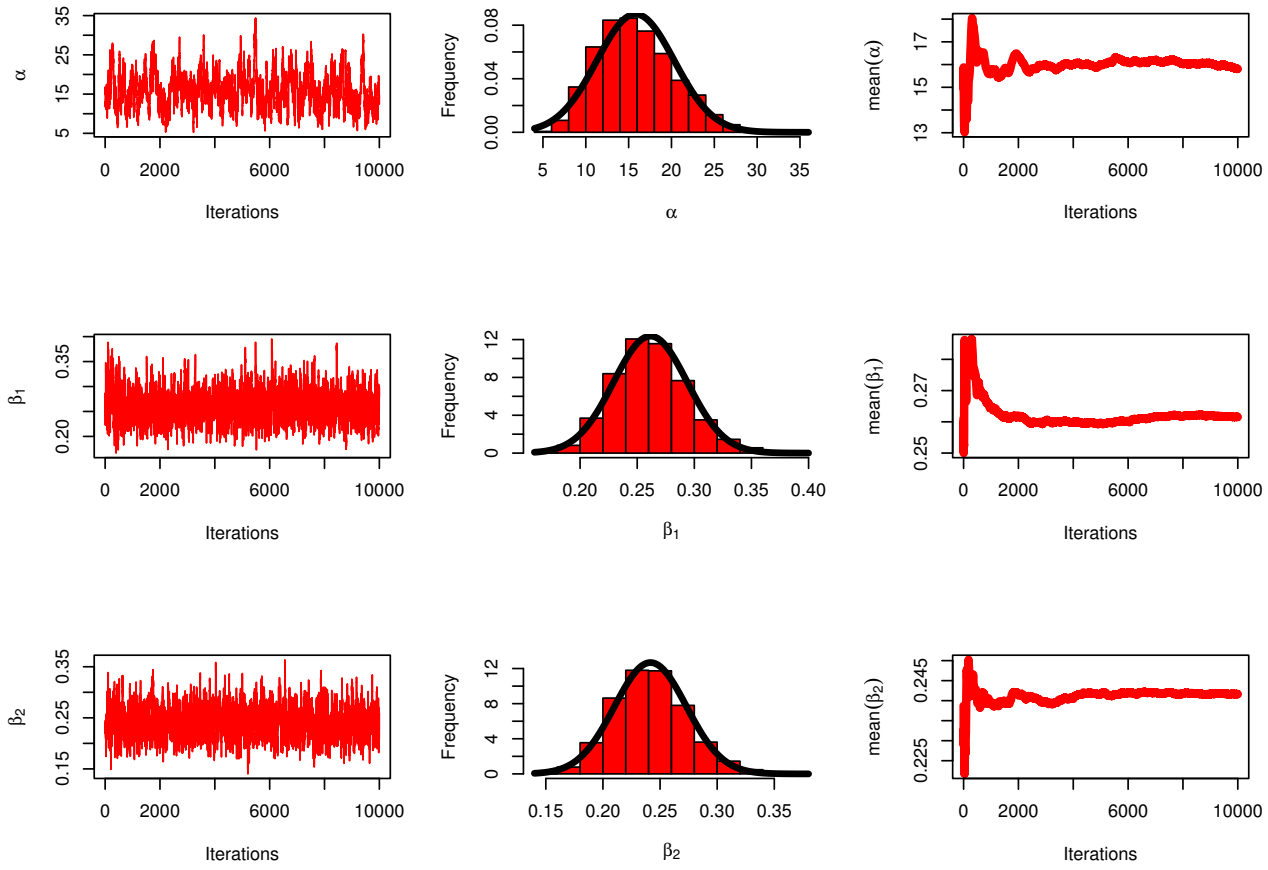

Figure 7. Trace plots and posterior density estimates of the parameters α, β_1, and β_2 obtained under Sample 3 of real data.

7. Conclusions

This study establishes a comprehensive inferential framework for the GLD under progressive Type-II censoring in the presence of competing risks. By developing both classical and Bayesian estimation procedures tailored to progressively censored competing risks settings, the proposed methodology addresses a notable gap in the existing literature and extends the applicability of the GLD model to survival analyses involving multiple failure mechanisms and incomplete lifetime information. The resulting maximum likelihood estimators, along with Bayesian estimators obtained under various loss functions, are demonstrated to be computationally feasible and statistically reliable across a broad range of censoring schemes and sample size configurations.

Extensive simulation studies provide compelling evidence of the favorable finite-sample performance of the proposed estimators, with Bayesian methods exhibiting particularly robust behavior. The empirical data analysis further substantiates the practical relevance of the GLD, highlighting its capacity to deliver interpretable and well-fitting models in reliability and biostatistical applications.

Collectively, the theoretical contributions and empirical results presented herein position the GLD as a flexible and competitive alternative for modeling progressively censored competing risks data. By introducing effective and reliable parameter estimation techniques, this work promotes the broader adoption of the GLD model in modern survival analysis. Potential avenues for future research include extensions to regression-based formulations, accelerated failure time frameworks, and joint modeling strategies, which would further enhance the model's utility for complex lifetime data encountered in engineering, biomedical research, and related applied domains.

Author contributions

M. H. Abu-Moussa: Conceptualization, resources, software, writing–review & editing, methodology, visualization; Ehab M. Almetwally: Project administration, resources, software, visualization, writing–review & editing; Abd El-Raheem M. Abd El-Raheem: Writing–original draft, methodology, visualization, conceptualization, resources, software. All authors have read and approved the final version of the manuscript for publication.

Use of Generative-AI tools declaration

The authors declare they have not used Artificial Intelligence (AI) tools in the creation of this article.

Funding statement

This work was supported and funded by the Deanship of Scientific Research at Imam Mohammad Ibn Saud Islamic University (IMSIU) (grant number IMSIU-DDRSP2602).

Conflict of interest

All authors declare no conflicts of interest in this paper.

References

1. A. M. Abd El-Raheem, M. Hosny, M. H. Abu-Moussa, On progressive censored competing risks data: Real data application and simulation study, *Mathematics*, **9** (2021), 1805. https://doi.org/10.3390/math9151805
2. S. A. Salem, O. E. Abo-Kasem, A. A. Khairy, Inference for generalized progressive hybrid type-ii censored weibull lifetimes under competing risk data, *Comput. J. Math. Statist. Sci.*, **3** (2024), 177–202. https://doi.org/10.21608/CJMSS.2024.256760.1035
3. R. Al-Jarallah, M. Ghitany, D. Kundu, Bayesian inference on gompertz-lindley distribution based on different loss functions, *Int. J. Appl. Math.*, **37** (2024), 187–204. http://dx.doi.org/10.12732/ijam.v37i2.5
4. F. Almathkour, A. Alothman, M. Ghitany, R. C. Gupta, J. Mazucheli, A comparative study of various methods of estimation for gompertz-lindley distribution, *Int. J. Appl. Math.*, **35** (2022), 347. https://doi.org/10.12732/ijam.v35i2.12

5. E. M. Almetwally, Uncertainty in lifetime data quantified with bayesian adaptive hamiltonian methods, *Measurement*, **276** (2026), 121455. https://doi.org/10.1016/j.measurement.2026.121455
6. E. M. Almetwally, Statistical inference for a one-parameter lifetime model under unified progressive hybrid censoring with binomial random removals, *AIMS Math.*, **11** (2026), 211–242. https://doi.org/10.3934/math.2026009
7. E. M. Almetwally, A. H. Tolba, D. A. Ramadan, N. Sayed-Ahmed, Comparative analysis of three distributions under studying the regression competing risks model with hiv to aids infection application, *Appl. Math. Inf. Sci.*, **19** (2025), 921–944. https://doi.org/10.18576/amis/190417
8. N. Balakrishnan, R. Aggarwala, *Progressive censoring: theory, methods, and applications*, Springer Science & Business Media, 2000.
9. N. Balakrishnan, E. Cramer, *Art of progressive censoring*, New York: Springer Science & Business Media, 2014. https://doi.org/10.1007/978-0-8176-4807-7
10. D. R. Cox, The analysis of exponentially distributed life-times with two types of failure, *J. Roy. Stat. Soc. B*, **21** (1959), 411–421. https://doi.org/10.1111/J.2517-6161.1959.TB00349.X
11. M. J. Crowder, *Classical competing risks*, New York: Chapman and Hall/CRC, 2001. https://doi.org/10.1201/9781420035902
12. S. O. A. El-Azeem, M. H. Abu-Moussa, M. M. M. El-Din, L. S. Diab, On step-stress partially accelerated life testing with competing risks under progressive type-ii censoring, *Ann. Data Sci.*, **11** (2024), 909–930. https://doi.org/10.1007/s40745-022-00454-0
13. R. B. Geskus, *Data analysis with competing risks and intermediate states*, New York: Chapman and Hall/CRC, 2015. https://doi.org/10.1201/b18695
14. M. E. Ghitany, S. M. Aboukhamseen, A. A. Baqer, R. C. Gupta, Gompertz-lindley distribution and associated inference, *Commun. Stat. Simul. C.*, **51** (2022), 2599–2618. https://doi.org/10.1080/03610918.2019.1699113
15. H. Haj Ahmad, E. M. Almetwally, D. A. Ramadan, Competing risks in accelerated life testing: A study on step-stress models with tampered random variables, *Axioms*, **14** (2025), 32. https://doi.org/10.3390/axioms14010032
16. A. Hassan, S. Maiti, R. Mousa, N. Alsadat, M. Abu-Moussa, Analysis of competing risks model using the generalized progressive hybrid censored data from the generalized lomax distribution, *AIMS Math.*, **9** (2024), 33756–33799. https://doi.org/10.3934/math.20241611
17. A. S. Hassan, R. M. Mousa, M. H. Abu-Moussa, Analysis of progressive type-II competing risks data, with applications, *Lobachevskii J. Math.*, **43** (2022), 2479–2492. https://doi.org/10.1134/S1995080222120149
18. A. S. Hassan, R. M. Mousa, M. H. Abu-Moussa, Bayesian analysis of generalized inverted exponential distribution based on generalized progressive hybrid censoring competing risks data, *Ann. Data Sci.*, **11** (2024), 1225–1264. https://doi.org/10.1007/s40745-023-00488-y
19. J. D. Kalbfleisch, R. L. Prentice, *The statistical analysis of failure time data*, John Wiley & Sons, 2002. https://doi.org/10.1002/9781118032985
20. A. Koley, D. Kundu, On generalized progressive hybrid censoring in presence of competing risks, *Metrika*, **80** (2017), 401–426. https://doi.org/10.1007/s00184-017-0610-9

21. A. Koley, D. Kundu, Analysis of progressive type-II censoring in presence of competing risk data under step stress modeling, *Stat. Neerl.*, **75** (2021), 115–136. https://doi.org/10.1111/stan.12226

22. D. Kundu, N. Kannan, N. Balakrishnan, Analysis of progressively censored competing risks data, *Handbook of Statistics*, **23** (2003), 331–348. https://doi.org/10.1016/S0169-7161(03)23018-2

23. A. K. Mahto, C. Lodhi, Y. M. Tripathi, L. Wang, Inference for partially observed competing risks model for kumaraswamy distribution under generalized progressive hybrid censoring, *J. Appl. Stat.*, **49** (2022), 2064–2092. https://doi.org/10.1080/02664763.2021.1889999

24. S. G. Nassr, E. M. Almetwally, W. S. A. El Azm, Statistical inference for the extended weibull distribution based on adaptive type-ii progressive hybrid censored competing risks data, *Thail. Statist.*, **19** (2021), 547–564.

25. M. Pintilie, *Competing risks: a practical perspective*, John Wiley & Sons, 2006. https://doi.org/10.1002/9780470870709

26. D. A. Ramadan, E. M. Almetwally, A. H. Tolba, Statistical inference to the parameter of the akshaya distribution under competing risks data with application hiv infection to aids, *Ann. Data Sci.*, **10** (2023), 1499–1525. http://doi.org/10.1007/s40745-022-00382-z

27. L. Tierney, J. B. Kadane, Accurate approximations for posterior moments and marginal densities, *J. Am. Stat. Assoc.*, **81** (1986), 82–86. https://doi.org/10.1080/01621459.1986.10478240

28. S. Yang, D. Meng, H. Wang, C. Yang, A novel learning function for adaptive surrogate-model-based reliability evaluation, *Philos. Trans. A Math. Phys. Eng. Sci.*, **382** (2024), 20220395. https://doi.org/10.1098/rsta.2022.0395

29. S. Yang, D. Meng, M. Alfouneh, B. Keshtegar, S. P. Zhu, A robust-weighted hybrid nonlinear regression for reliability based topology optimization with multi-source uncertainties, *Comput. Method. Appl. M.*, **447** (2025), 118360. https://doi.org/10.1016/j.cma.2025.118360

30. S. Yang, D. Meng, H. Yang, B. Keshtegar, A. M. De Jesus, S. P. Zhu, Adaptive kriging-assisted enhanced sparrow search with augmented-lagrangian first-order reliability method for highly efficient structural reliability analysis, *Reliab. Eng. Syst. Safe.*, **267** (2025), 111916. https://doi.org/10.1016/j.ress.2025.111916

AIMS Press